

DEVELOPMENT AND SIMULATIONS OF AIRCRAFT GUIDANCE SYSTEM USING A 3-DEGREE-OF-FREEDOM POINT MASS MODEL

Martins Sudars

*Aviation Institute of Riga Technical University, Lomonosova 1, Riga, LV-1019
E-mail: msudars@yahoo.com*

Received 16 January 2009; accepted 5 May 2009



Martins SUDARS, Msc Eng

Education: Msc Eng Degree in Aeronautics from Aviation Institute, Riga Technical University, 2007.

Research Interest: advanced and intelligent flight control systems, GNC of UAVs, Flight mechanics of atmospheric and exatmospheric flight, re-entry vehicles.

Publications: author and co-author of five publications.

Present Position: PhD candidate at Aviation Institute of Riga Technical University, Latvia.

Abstract. Numerical simulations play an essential role in the development and testing of navigation and guidance algorithms, especially when developer must keep the development costs as low as possible. Low budget development focuses mainly on utilization of numerical flight mechanics simulators including optimization and hardware in loop tests. Reliable, high fidelity results can be easily obtained by numerical simulations of flight dynamics utilizing computing power provided by a normal off-the-shelf home PC. However, it still requires a simple, but good and valid model of the aircraft and environment. This paper describes an approach to a numerical simulation of aircraft motion that respects the requirement for a full environment high fidelity model and keeps a good interface for further development of attitude control. The goal is achieved by directly specifying the aerodynamic angles of the vehicle in the simulation environment by the guidance system, which can later be used as input for attitude control algorithms. It is proved how an appropriate selection of reference frames and formulation of laws of motion gives very quick and reliable results by employing large integration time steps that would be difficult to achieve in 6-degree-of-freedom simulations. This paper also investigates the range of applicability, advantages, and drawbacks of this method. An example of an aerodynamic angle-based guidance law for a UAV is explained and demonstrated by figures.

Keywords: Numerical simulations, trajectory, point mass model, aerodynamic angles, guidance, navigation, UAV flight simulations.

1. Introduction

Often navigation, guidance and control systems are developed separately and may even be accommodated on separate hardware units. For small aircraft like UAVs, the function of all three systems can be effectively merged into one single flight computer, but practice shows that separate engineers nevertheless develop in separate blocks or the algorithms of those systems.

To test navigation and guidance algorithms and carry out hardware-in-loop simulations of navigation

hardware, a sophisticated model of the aircraft and environment has to be built. Compared to full 6-degree-of-freedom motion models, point mass models allow state integration with a much larger time step, thus requiring lower computing power, but providing high accuracy results. Another important aspect in favour of point mass model utilization is usually the limited availability of aerodynamic data and control actuator specifications required for the 6DOF model. For the point mass model the vehicle's attitude is given as an input.

In order to avoid numerical problems and simplify

equations of motion, the simulation environment features equations of motion in the Cartesian coordinate system. A special set of transformations has to be applied in order to convert a vehicle's forces from body fixed reference frame to an inertial frame where integration of states takes place.

If the vehicle's attitude response information is approximately known (natural frequency, rate damping), it is possible to easily implement the effect of those characteristics in form of a state filter between commanded attitude and attitude output port from the guidance system. In this way, a point mass model becomes a perfect testbed for navigation and control system development and testing.

2. Guidance and navigation of vehicles

A navigation system utilizes certain measurable states in order to compute the other states.

Guidance and flight control systems may be virtually separated from each other, first considering inputs from navigation systems and giving orders to the flight control system, which takes care of an airplane's attitude by controlling the aerodynamic actuators and high lift devices (and the propulsion system).

Outputs of the guidance system-angle of attack, aerodynamic bank angle, and angle of slip – are sufficient to control the aircraft's trajectory. In case of exatmospheric vehicles, the attitude with respect to local horizon and inertial reference frames may also become significant.

The guidance system may also be partially responsible for high lift device control in the form of acceleration control or simply by help of some built-in logic, which, for instance, gives an order to activate high lift devices in takeoff and landing phases.

3. Manoeuvres and performance

This chapter illustrates that just just controlling flight path angle and heading in NED reference frame may achieve the goals of the guidance system. In some cases, velocity control must also be considered in order to keep certain aerodynamic characteristics.

Let us consider the basic equations of flight performance and manoeuvring.

4. Flight path angle control

For a general case if we neglect gravity, the flight path changes once a force perpendicular to the flight direction has been applied:

$$\dot{\gamma} = \omega_{fp} = \frac{L}{v} \quad (1)$$

In a realistic case, a gravity force bias exists and only excess lift can produce a change in the flight path angle. The following equation has no analytic solution and must be solved numerically inside the simulation.

$$\dot{\gamma} = \frac{L - W \sin \gamma}{v} \quad (2)$$

This gravity component should be included as bias inside the guidance loop in order to provide equal control authority at various flight path angles.

The lift force depends on states like dynamic pressure and angle of attack, which usually defines the lift coefficient according to the polars:

$$L = 0,5 C_L S \rho v^2$$

where $C_L = f(\alpha)$

and can usually be expressed as a linear relationship:

$$C_L = C_{L0} + C_{L\alpha} \alpha$$

for a typical wing, so that α can be used directly inside the loop in order to control $\dot{\gamma}$.

5. Bank angle control and turns

In a level turn, the balance of the force in a turn is given by the following equations (Bandu 1998; Filippone 2006; Narayan *et al.* 2008; Schmidt 1998).

Along normal:

$$L \cos(\phi_A) - W = 0;$$

Along binormal:

$$L \sin(\phi_A) = m \frac{v^2}{R_{turn}} \quad (3)$$

$$\text{or } L \sin(\phi_A) - \frac{W v^2}{g R_{turn}} = 0;$$

The change in the flight path heading:

$$\dot{\chi} = \frac{v}{R_{turn}} = \frac{W L \sin(\phi_A)}{v g} = \frac{L \sin(\phi_A)}{v m}; \quad (4)$$

or

$$\dot{\chi} = \frac{g}{v} \tan^2(\phi_A);$$

In general the equations of motion (Narayan *et al.* 2008):

Along the flight path:

$$T \cos \beta - D - W \sin \gamma = 0;$$

Along its normal:

$$L \cos \phi_A - W \cos \gamma = 0;$$

Along its binormal:

$$T \sin \beta + L \sin \phi_A - m \frac{v^2}{R_{turn}} \cos^2 \gamma = 0 \quad (5)$$

$$\text{or } T \sin \beta + L \sin \phi_A - \left(\frac{W v^2 \cos^2 \gamma}{g R} \right) = 0;$$

Resulting law for heading control (Filippone 2006):

$$\dot{\chi} = \frac{v}{R_{turn}} \cos \gamma = \frac{L \sin(\phi_A) + T \sin \beta}{m v \cos \gamma} \quad (6)$$

Note: heading as definition of flight path direction loses meaning near vertical climb or dive due to singularity.

The equations prove that the bank angle can be directly used to control the heading of the aircraft, but rate of heading will also depend on angle of attack.

Use of high-lift devices and simulation of their effect is also possible by point mass simulation. High-lift

devices such as flaps and slats usually produce the specific value of ΔC_L , ΔC_D and ΔC_M . ΔC_M is not an input for the point mass simulation, but it may change the trimmed α , and that effect should be considered inside the guidance and control law.

6. Attitude control inside the point mass model

The trajectory of a vehicle assumed as point mass depends on various perturbances, and the most significant are aerodynamic forces, gravity, and the thrust force produced by the power plant. Aerodynamic forces depend on the vehicle's relative motion with respect to the atmosphere (co-rotating with the earth), wind, and wind gusts (thermals, microbursts, rotors, and other turbulence). If the attitude is constrained by given aerodynamic angles, the aerodynamic and propulsive forces must be converted to an inertial or earth-fixed reference frame by a set of transformations.

7. Reference frames and force conversions

The aerodynamic attitude of the aircraft is described by angle of attack and angle of slip, which relates the body reference frame with the wind axis coordinate system by the transformation matrix T_{BW} . Aerodynamic attitude has no direct relation with local horizon or any other planet-fixed reference frame (Fig 1).

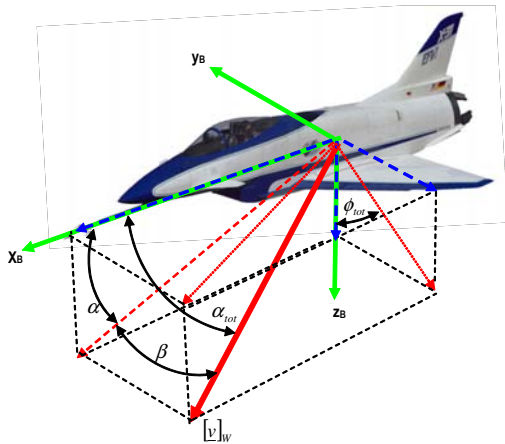


Fig 1. Definition of aerodynamic angles used for attitude definition on relative wind reference frame (Zipfel 2001)

$$T_{BW} = \begin{bmatrix} \cos(\alpha)\cos(\beta) & -\sin(\alpha)\cos(\beta) & -\sin(\alpha) \\ \sin(\beta) & \cos(\beta) & 0 \\ \sin(\alpha)\cos(\beta) & -\sin(\alpha)\sin(\beta) & \cos(\alpha) \end{bmatrix} \quad (7)$$

Aerodynamic bank angle describes a vehicle's attitude with respect to the relative wind velocity vector and the local horizon plane. Only one roll angle is sufficient to relate the wind coordinate system with the velocity reference frame (it is vehicle carried reference frame which is always aligned with the velocity vector in NED frame) (Fig 2) (Sudars 2008a).

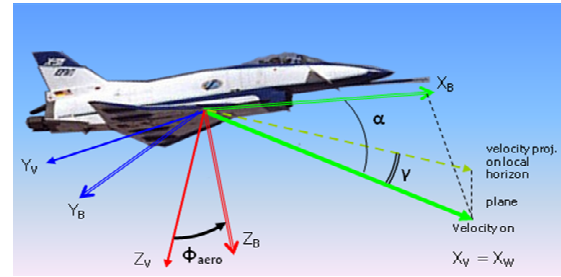


Fig 2. Definition of the velocity fixed reference frame (V or VEL) and the attitude of the vehicle with respect to it. In this figure, no wind and wind gust presence is assumed in order to better illustrate relation with body frame (B)

Transformation matrix:

$$T_{WV} = \begin{bmatrix} 1 & 0 & 0 \\ 0 & \cos(\phi_A) & \sin(\phi_A) \\ 0 & -\sin(\phi_A) & \cos(\phi_A) \end{bmatrix} \quad (8)$$

If only angle of attack and aerodynamic bank angle is utilized for flight control inside the model, the slip angle is assumed 0, meaning the flight is assumed to be perfectly coordinated. In that case, the longitudinal aerodynamic model of the vehicle is completely sufficient (Regan 1984).

$$T_{BW} = T_{BW}T_{WV} \quad (9)$$

$$T_{VN} = \begin{bmatrix} \cos(\gamma)\cos(\chi) & \cos(\gamma)\sin(\chi) & -\sin(\gamma) \\ \sin(\chi) & \cos(\chi) & 0 \\ \sin(\gamma)\cos(\chi) & \sin(\gamma)\sin(\chi) & \cos(\gamma) \end{bmatrix} \quad (10)$$

where

$$\gamma = \arcsin\left(\frac{\dot{h}}{v_{hor}}\right) = \left(\frac{-w_N}{\sqrt{u_N^2 + v_N^2}}\right)$$

$$\chi = \arctan 2(u_N, v_N)$$

Body-to-NED relation:

$$T_{BN} = T_{BV}T_{VN} \quad (11)$$

8. Computation of relative wind velocity vector

Relative wind speed computation takes into account wind speed with respect to NED and wind gust speed with respect to NED.

$$[\vec{v}]_W = [\vec{v}]_N + [\vec{v}_W]_N + [\vec{v}_{Gust}]_N \quad (12)$$

The resulting vector $[\vec{v}]_W$ defines the reference direction for attitude specified by aerodynamic angles.

9. Equations of motion

The synthetic environment utilizes Newton's 2nd law in the Cartesian coordinate system fixed to the inertial reference frame:

$$\frac{d^2 [\vec{r}]_i}{dt^2} = \frac{\sum F}{m} \quad (13)$$

where $\sum F$ designates all modelled forces applied to the vehicle: aerodynamic, propulsive and gravity forces.

10. State integration

When the Cartesian coordinate system is utilized, states can usually be integrated with respect to a local reference frame (like runway fixed frame) or a global frame like ECI. The experiment described in the example utilized a full environment simulation tool working in ECI frame (J2000 epoch) (Sudars 2008b).

11. Implementation

The approach described can be implemented in any synthetic environment. Because the flight states are known, the forces produced can be easily converted by the previously mentioned conversion matrices (Fig 3).

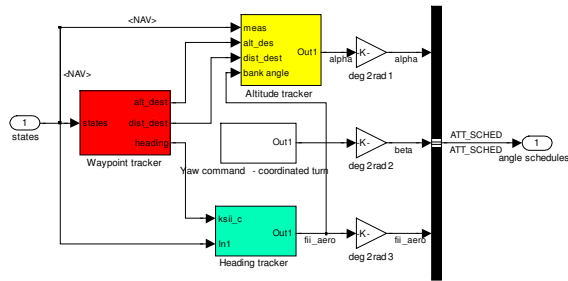


Fig 3. Guidance law implemented in a Simulink model. The output of the law are aerodynamic angles that are fed to the kinematic conversion block in the point mass synthetic environment to produce conversion matrices T_{BW} and T_{VW}

12. Advantages and drawbacks

Since the attitude of the vehicle has been fixed to the relative wind velocity vector, rapid changes in that vector would cause the vehicle to make an abrupt change of attitude that may not correspond to a real situation. The model is therefore not valid for stalls, spins, bell manoeuvres, etc. but can be applicable to rolls, loops, etc., where velocity vector changes its direction much more gradually.

Wind gusts would cause rapid changes in attitude. In order to avoid these effects, the wind gust model should not be applied. The model works well with the constant wind model or changing wind with small time and space derivative. Here an alternative solution exists—separating relative wind vectors and utilizing the wind gust vector only for residual lift computation, but it does not have any good practical application.

Forces related to or originating from short period dynamics have been ignored.

13. Range of applications

The methodology mentioned has a certain range of applications. Some problems may be experienced when

trajectory approaches singularity at flight path angle $\gamma = 90^\circ$ or $\gamma = -90^\circ$. At these conditions, the aerodynamic bank angle cannot be specified. If the natural behaviour of the aircraft is to be kept, the bank angle jump has to be prevented by fixing the yaw angle with respect to the NED reference frame at the moment the flight path angle touches near $\gamma = 90^\circ$ or $\gamma = -90^\circ$.

14. Simulation of UAV’s guidance algorithm

The example given combines two tasks: control of velocity vector direction and following a certain predefined route specified by waypoints the vehicle must fly over at a given altitude. The vehicle must also maintain a given relative airspeed by adjusting the throttle.

The vehicle utilized was a generic model of a UAV representing an approximate model of a vehicle being developed at RTU Aviation Institute. The Simulink model has been utilized for FCS development in RTU Aviation Institute.

The attitude and velocity control laws considered in this UAV guidance example resulted in the trajectory given by the figures in this chapter (Figs 4–17).

Simulation utilized:

Time step of simulation: 1 second

Solver: Runga-Kutta ODE4;

Total time: 1880 sec (~ 31 min 20 sec).

State integration: ECI reference frame, Cartesian coordinate system.

Altitude control

Altitude control is done by control of the flight path angle (most common way in general aviation). This guidance law is simple:

$$\gamma_{des} = \arctan\left(\frac{h_g - h_{meas}}{d_{range}}\right)$$

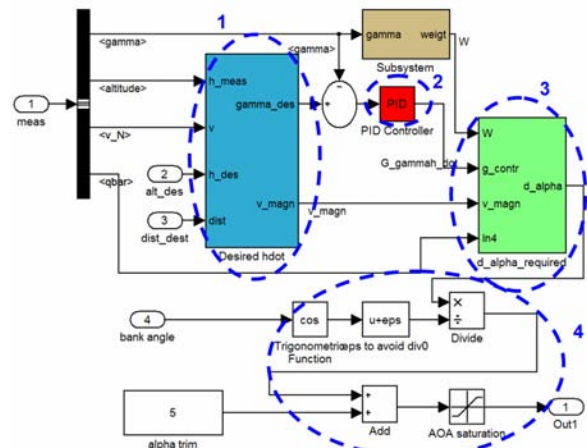


Fig 4. Vertical guidance algorithm designed in Simulink environment. Its main components: 1—desired flight path angle computation, 2—PID for flight path angle rate control, 3—computation of lift increment, expressed as AOA increment 4—final AOA output, taking into account bank angle and trim angle of attack of level flight

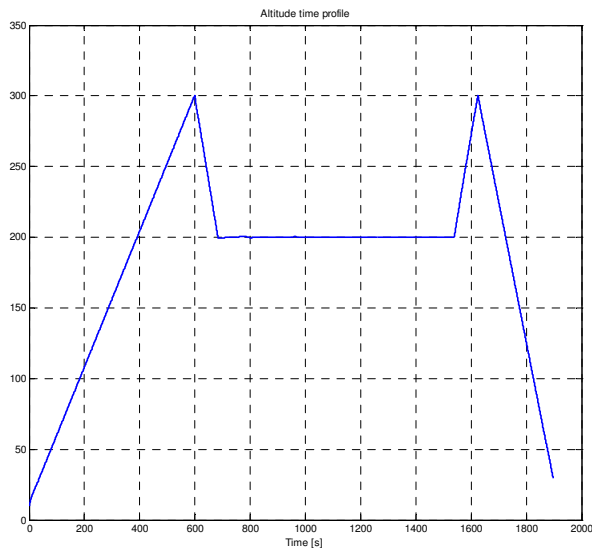


Fig 5. Altitude time profile. Altitude has been specified by user for each of the waypoints. The aircraft performed gradual altitude gain and descent

	lat	long	alt	place
init	57.15177	24.40836	10	Ādažu poligons
route	57.31	24.44	300	pie skultes
	57.32129	24.40536	200	zvejniekciems
	57.31656	24.40587	200	
	57.30478	24.40613	200	
	57.29697	24.40712	200	
	57.28629	24.41202	200	
	57.27242	24.41181	200	
	57.26266	24.40827	200	
	57.25319	24.40373	200	
	57.24303	24.39737	200	
	57.23067	24.38555	200	
	57.21357	24.36553	200	pie lilastes
	57.2025	24.34974	200	
	57.18665	24.32399	200	
	57.1605	24.26665	200	
	57.1564	24.2573	200	
57.14169	24.24048	200	pie carnikavas	
57.13652	24.27558	300		
final	57.15049	24.40742	30	Ādažu poligons

Fig 6. Definition of a generic UAV's route by specifying waypoints and flyover altitude

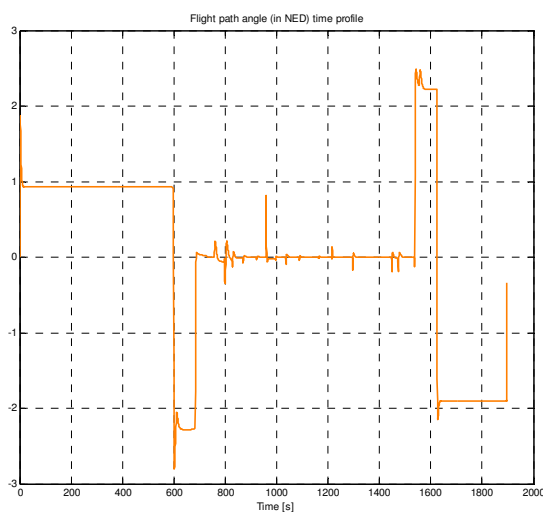


Fig 7. Flight path angle to satisfy altitude requirements specified by user

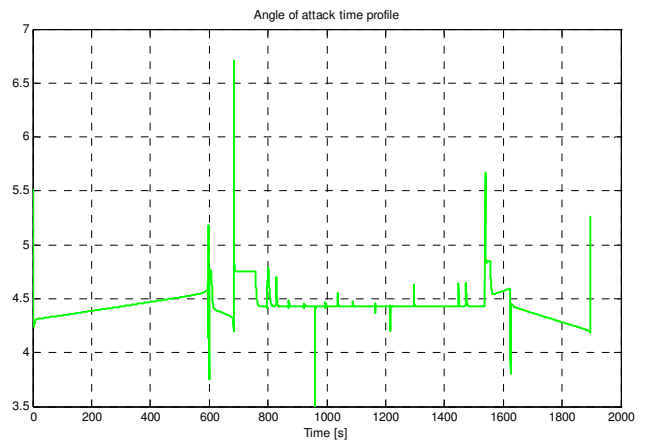


Fig 8. Angle of attack time profile. Angle of attack peaks are used to compensate for lift losses during banks

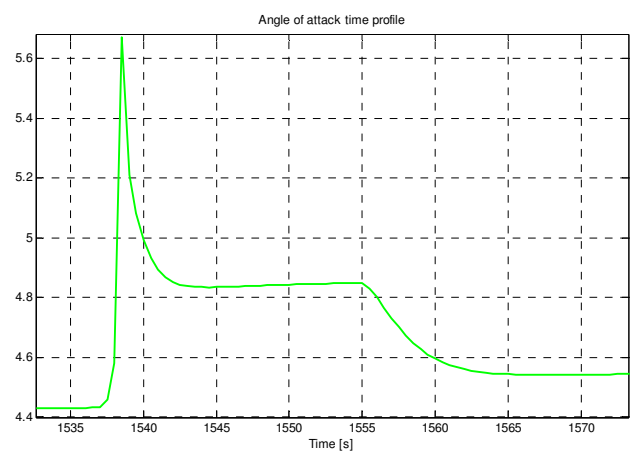


Fig 9. Zoom-in illustration of angle of attack

Heading control

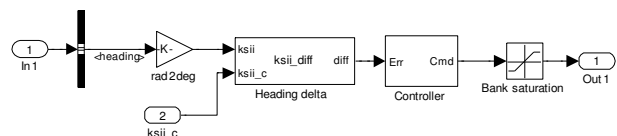


Fig 10. Simple heading and bank angle control algorithm

The model described features very simple heading control; bank angle is obtained by PID controller from heading error. Since $\chi \sim \phi_A$ at small angles of ϕ_A and the flight path angle is not steep, a PID controller can be utilized directly between heading error and output aerodynamic bank angle. This approach is valid for ascents and descents that are not steep (<10 deg). For the simulation, the maximum bank angle has been limited to 15 degrees, which is a reasonable limit for aerial photography.

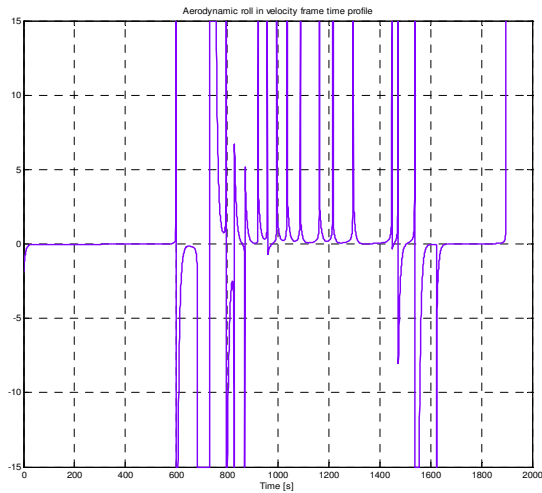


Fig 11. Aerodynamic bank angle as requested by the guidance system's algorithm. In most of the curves, the algorithm uses the maximum allowed bank angle (30 degrees) to more quickly align the heading with the direction that leads to the next waypoint

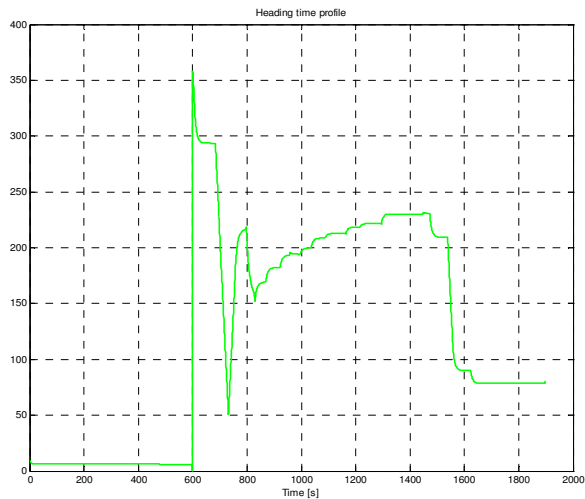


Fig 12. Heading time profile as a result of the aerodynamic bank

Velocity control

Velocity control has been implemented as a simple controller that maintains airspeed specified by a time schedule. The integral coefficient of the PID plays a major role in velocity control.

In this example, velocity is maintained constant, but can be adapted to provide maximum rate of climb, higher rate of sink, etc.

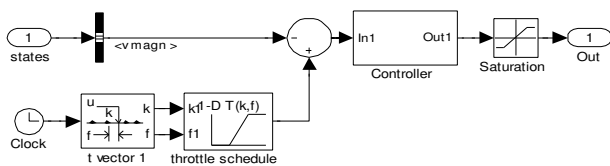


Fig 13. A very simple PID-based velocity control. Maintains given airspeed by opening/closing throttle. Desired airspeed obtained from lookup table prepared by user

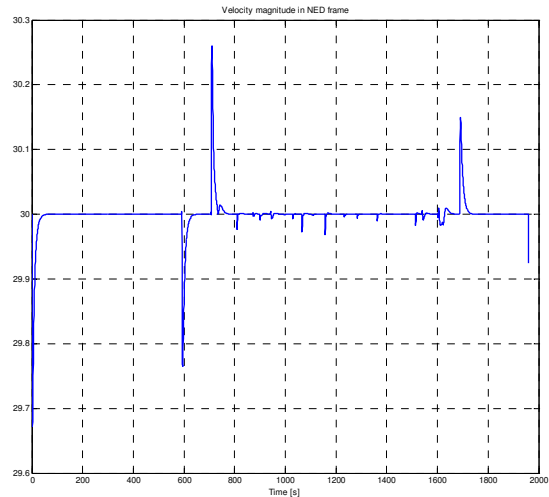


Fig 14. Velocity magnitude (ground speed) in NED reference frame. Ground speed matches wind speed in absence of wind

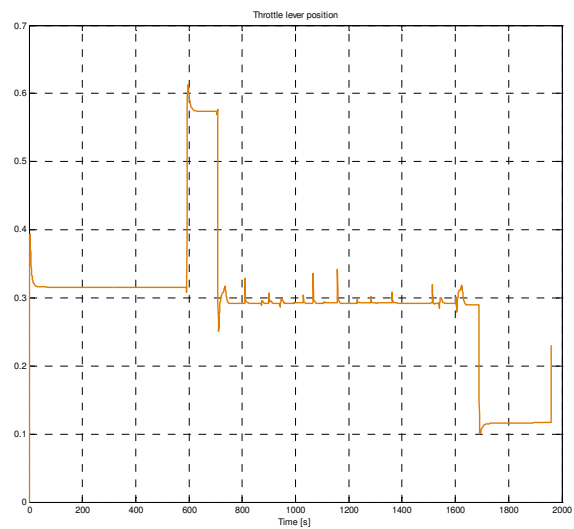


Fig 15. Throttle lever position is controlled by processing measured and given airspeed

Trajectory

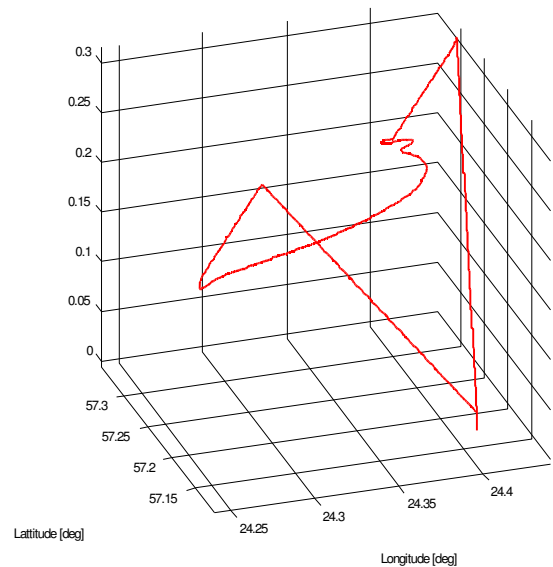


Fig 16. 3D illustration of the flight trajectory. Axes are not proportional

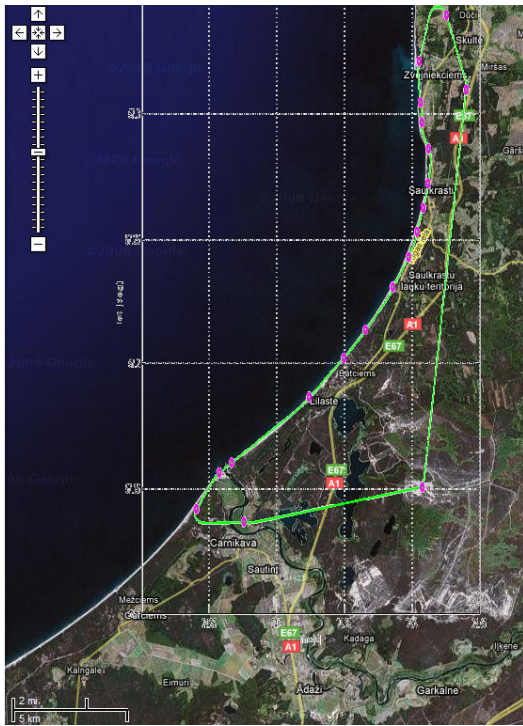


Fig 17. Defined waypoints (magenta circles) and the ground track of the UAV vehicle following a route along the coastline (green). Ground track plotted on a map provided by Google Maps

15. Effect of the timestep size on error and computation time

Let us consider a slightly different simulated flight with a different altitude profile.

The simulation was performed in the Matlab 2008a environment on the Windows Vista Business platform by a Fujitsu-Siemens E8410 computer (Intel T7500 processor).

- Real mission time: 1981.5 seconds
- Elapsed sim. time with $\Delta t=1$ sec: 3.486340 sec.
- Elapsed sim. time with $\Delta t=0.1$ sec: 30.081938 sec.

A larger simulation time step does not allow translation dynamics of the vehicle and guidance controller to be captured and may result in highly oscillating or unstable behaviour (Figs 18–23).

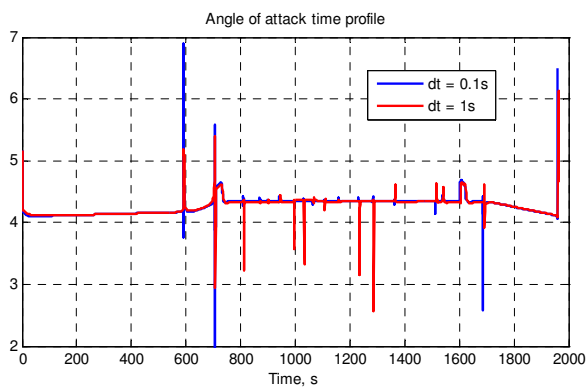


Fig 18. Time profiles of guidance system’s requested angle of attack for integration with two different time steps

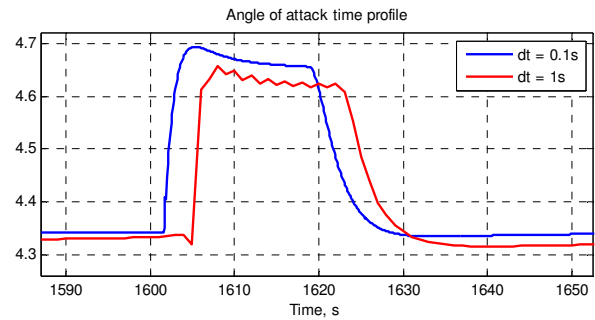


Fig 19. Zoom-in figure of plots in Fig 18. Visible shift approximately 3 sec

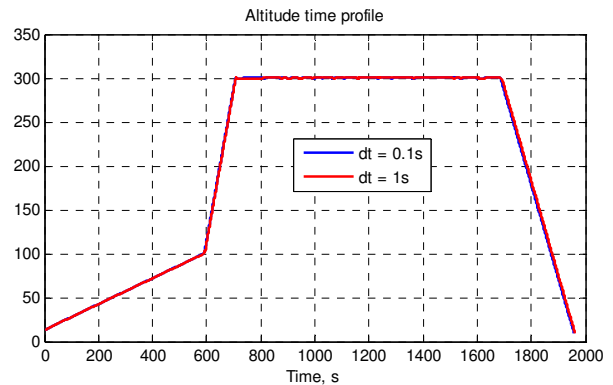


Fig 20. Altitude profiles for simulations with different time steps

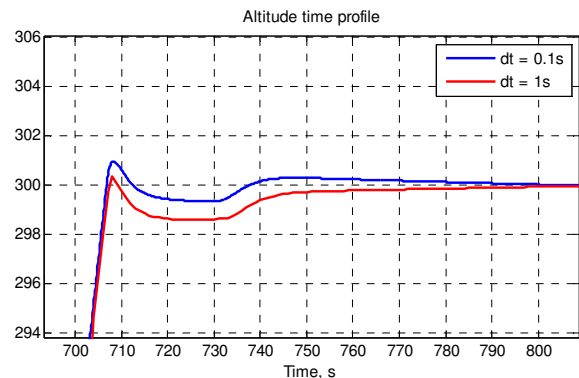


Fig 21. Altitude profiles at the moment of reaching the cruise altitude of 300 m

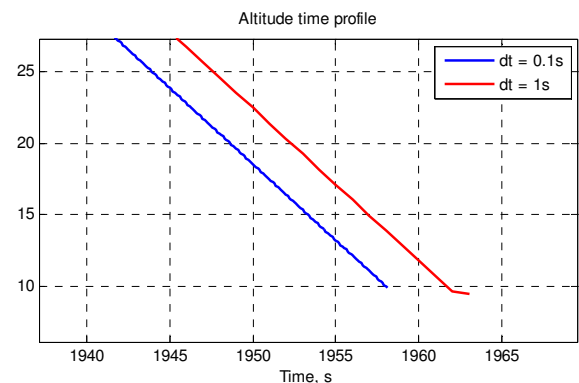


Fig 22. Altitude profiles at end of the mission, illustrating the actual difference caused by different time steps of the ODE4 integration

The relative error of the simulated mission duration was between $\Delta t=0.1$ and $\Delta t=1$ sec: $\epsilon_{rel} = 0.20 \%$.

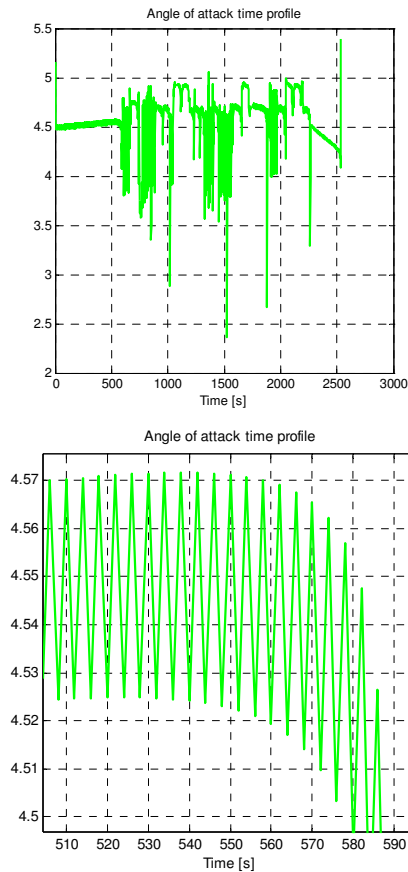


Fig 23. Angle of attack time profile (above) and zoomed magnified picture (below) when simulated with an integration timestep that is too large: 2 sec. The integrator does not capture important events and keeps oscillation around equilibrium

16. Conclusions

This paper and the given example illustrated the efficiency and advantages of vehicle dynamic's simulations in form of a point mass body with its attitude specified in the described velocity reference frame. It is particularly suitable for simulations of airplane, airship, missile, or a re-entry vehicle.

The method allows directly specifying the attitude of the vehicle with respect to the relative wind velocity vector and local horizon, which makes it very suitable for trajectory computations even with a limited aerodynamic database available. The method allows assuming perfectly coordinated turns or specifying any other angle of slip for any particular purpose.

This kind of simulation is limited to vehicles that are not facing strong wind gusts or performing aerobatic manoeuvres or other manoeuvres involving rapid changes of velocity vector direction. However, for most aircraft and entry vehicles, it is a quick and high fidelity approach to the simulation.

The method is particularly suitable for integration in simulation environments utilizing the Cartesian coordinate system for state integration.

The method can be utilized inside the vehicle's onboard computer for online trajectory estimation and optimization.

Symbols and acronyms

Symbols

C_D – drag coefficient

C_L – lift coefficient

C_M – pitch moment coefficient

d_{range} – downrange to next waypoint

g – gravity acceleration at given altitude, latitude and longitude

h – altitude

h_{fg} – flyover altitude of the next point

h_{meas} – measured altitude

L – lift force

m – mass

R_{turn} – radius of turn

T_{AB} – transformation matrix from reference frame A to B

u_A – x velocity in reference frame A

V – velocity in given reference frame

W – weight

α – angle of attack

β – angle of slip

Δ – difference, increment (ΔC_x – increment of coefficient C_x)

γ – flight path angle in North-East-Down reference frame

γ_{des} – desired flight path angle

λ – longitude

μ – latitude

χ – flight path heading angle in North-East-Down reference frame

ϕ – roll angle with respect to NED reference frame

ϕ_A – aerodynamic bank angle with respect to local horizon

Indexes of vectors and matrices designating reference frames

B – body-fixed reference frame

E – Earth-Centred Earth-Fixed reference frame

I – Earth-Centred Inertial reference frame

N – North-East-Down reference frame

V – relative velocity-fixed reference frame

W – wind reference frame

Abbreviations

DOF – degrees of freedom

ECI – Earth-Centered Inertial (reference frame)

NED – North-East-Down (reference frame)

ODE – ordinary differential equation

PID – proportional-integral-derivative (controller)

UAV – unmanned aerial vehicle

VEL – velocity aligned reference frame

Note. This paper is based on the author's presentation entitled "Development and simulations of aircraft guidance system using a 3-degree-of-freedom point mass

model” and made at a scientific conference at Riga Technical University Aviation Institute on 13.10.2008 in Riga, Latvia.

References

Bandu, P. N. 1998. Performance, stability, dynamics and control of airplanes. In *AIAA, United States*.

Filippone, A. 2006. *Performance of fixed and rotary wing aircraft, by elsavier aerospace engineering series*. United States.

Narayan, P.; Campbell, D.; Walker, R. 2008. Multi-objective UAS flight management in time constrained low altitude local environments. In *AIAA-2008-872*. Brisbane, Australia: Queensland University of Technology.

Regan, F. J. 1984. Reentry vehicle dynamics. In *AIAA, United States*.

Schmidt, L. V. 1998. Introduction in aircraft flight dynamics. In *AIAA*.

Sudars, M. 2008a. FMST user manual. In *Internal Document at BUSIT, Thales Alenia Space Italy, Turin*.

Sudars, M. 2008b. Simulink based tool for aerospace vehicle flight mechanics numerical simulations. In *Scientific Proceedings of Riga Technical University, Series 6 "Transport and Engineering. Transport. Aviation Transport"*, vol. 27. Riga: RTU.

Zipfel, P. H. 2001. Modeling and simulation of aerospace vehicle dynamics. In *AIAA, United States*.

SKRYDŽIO VALDYMO SISTEMOS KŪRIMAS IR MODELIAVIMAS NAUDOJANT MATERIALAUS TAŠKO MODELĮ SU TRIMIS LAISVĖS LAIPSNIAIS

M. Sudars

S a n t r a u k a

Straipsnyje pateiktas lėktuvo slenkamojo judesio dinamikos modeliavimo efektyvus ir patikimas metodas. Įvedus konkrečias koordinačių sistemas, šiuo metodu galima nustatyti aerodinaminius duomenis ir greičio atskaitos sistemą. Tai ypač naudinga modeliuojant skrydžio valdymo ir navigacijos algoritmus, nes čia nebūtinai visi aerodinaminiai duomenys. Šis metodas ir jo pritaikymas iliustruojamas BSA valdymo pavyzdžiu.

Reikšminiai žodžiai: skaitinis modeliavimas, trajektorija, modelio materialus taškas, aerodinaminiai kampai, valdymas, navigacija, BSA skrydžio modeliavimas.